12/6-27-94 (1)

ANL/ESD/TM-66

Characteristics and Computer Model Simulation of Magnetic Damping Forces in Maglev Systems

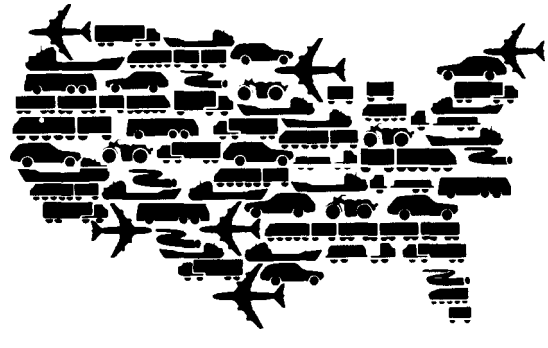

Center for Transportation Research

Argonne National Laboratory

Operated by The University of Chicago,
under Contract W-31-109-Eng-38, for the

United States Department of Energy

Argonne National Laboratory

Argonne National Laboratory, with facilities in the states of Illinois and Idaho, is owned by the United States Government, and operated by the University of Chicago under the provisions of a contract with the Department of Energy.

This technical memo is a product of Argonne's Energy Systems (ES) Division. For information on the division's scientific and engineering activities, contact:

Director, Energy Systems Division
Argonne National Laboratory
Argonne, Illinois 60439-4815
Telephone (708) 252-3724

Presented in this technical memo are preliminary results of ongoing work or work that is more limited in scope and depth than that described in formal reports issued by the ES Division.

Disclaimer

Reproduced directly from the best available copy.

Available to DOE and DOE contractors from the Office of Scientific and Technical Information, P.O. Box 62, Oak Ridge, TN 37831; prices available from (615) 576-8401.

Available to the public from the National Technical Information Service, U.S. Department of Commerce, 5285 Port Royal Road, Springfield, VA 22161.

ANL/ESD/TM-66

Characteristics and Computer Model Simulation of Magnetic Damping Forces in Maglev Systems

by J.L. He, D.M. Rote, and S.S. Chen

Center for Transportation Research, Energy Systems Division,
Argonne National Laboratory, 9700 South Cass Avenue, Argonne, Illinois 60439

May 1994

Work sponsored by United States Army Corps of Engineers and the Federal Railroad Administration through interagency agreements E8691R001 and DTFR 53-91-X-00018, respectively, with the United States Department of Energy and by Argonne National Laboratory

Contents

Table

Figures

Figures (Cont.)

Characteristics and Computer Model Simulation of Magnetic Damping Forces in Maglev Systems

by

J.L. He, D.M. Rote, and S.S. Chen

Abstract

This report discusses the magnetic damping force in electrodynamic suspension (EDS) maglev systems. The computer model simulations, which combine electrical system equations with mechanical motion equations on the basis of dynamic circuit theory, were conducted for a loop-shaped coil guideway. The intrinsic damping characteristics of the EDS-type guideway are investigated, and the negative damping phenomenon is confirmed by the computer simulations. The report also presents a simple circuit model to aid in understanding damping-force characteristics.

1 Introduction

An electrodynamic suspension (EDS) maglev system uses repulsive magnetic forces for levitation, propulsion, and guidance. These forces are produced by the interactions between the vehicle-borne superconducting magnets and the eddy currents that they induce in the nonferromagnetic conductors installed on the guideway.

The response of a maglev vehicle to periodic or transient disturbances, such as occur with discrete-coil guideway conductors, or guideway discontinuities and gusts of wind, is determined by the type of motion-control system that is employed. The motion-control system typically comprises the natural or intrinsic damping properties of the magnetic suspension system and any enhanced damping and control mechanisms, which may be active or passive in nature. Passive damping mechanisms include conducting plates (such as the walls of a cryostat) in which eddy currents induced by unwanted motion are dissipated, secondary suspension systems consisting of springs and dampers, and aerodynamic drag forces. Active motion-control mechanisms may include servo-controlled magnetic-field sources, propulsion-motor phase controls, aerodynamic control surfaces, active secondary suspension systems, and others.

It is well-known that the intrinsic damping provided by the interaction of the magnets with the guideway conductors is insufficient by itself to provide good ride quality. In fact, several investigators have shown that above a critical speed (generally of the order of 5 to 10 m/s), the intrinsic damping actually becomes negative. This being the case, additional damping must be utilized not only to provide suitable ride quality but also to ensure the vehicle's dynamic stability. Of course, any devices that must be added to enhance the intrinsic damping of the magnetic

suspension system increase both the complexity and the cost of the system design and may also adversely affect the energy efficiency. Consequently, the intrinsic damping characteristics of a magnetic suspension system have both technical and economic importance.

The damping-force characteristics of a single wire conductor moving above a thin sheet conductor were investigated on the basis of a Laplace-transform technique[1] and Fourier integral method.[2] In References 1 and 2, the authors concluded that a negative damping force exists in the vertical-motion mode when the longitudinal speed is higher than the critical speed. A confirming experiment was also reported in Reference 2. The damping-force characteristics of a loop-coil guideway were studied in Reference 3, where similar results were obtained by assuming a fundamental wave in longitudinal motion only. Both experimental and theoretical investigations of the damping characteristics of the null-flux, coil-suspension system were reported.[4,5] The influence of the persistent-current mode of superconducting magnets on magnetic damping force was reported in Reference 6. Recently, experimental work conducted at Argonne also has confirmed the intrinsic, negative magnetic damping phenomenon in a laboratory simulation of an EDS maglev system; in this work, a single magnet was forced to vibrate in a direction normal to the surface of a rotating aluminum drum.[7] In addition, magnetic damping problems are also discussed in References 8 and 9.

In spite of past efforts by several investigators, the precise nature of the intrinsic damping characteristics or, more generally, the motion-dependence of the magnetic forces in an EDS maglev system remains somewhat elusive. This is due, in part, to the relatively small magnitude of the motion-dependence, which allows it to be masked, in both laboratory and field experiments, by a variety of confounding effects. These effects include other damping mechanisms, such as mechanical damping of structural members, aerodynamic damping, and enhanced eddy-current damping in cryostat walls. In the case of laboratory experiments, especially, these damping effects may also include the constraints imposed by the nature of the experiment, such as the occurrence of other, stabilizing influences. This elusivity is also due to the considerable difficulty in computing these characteristics for a realistic system. To address such problems, computer models must be capable of handing both the relative velocity of one or more magnets with respect to a conductor array and an additional oscillatory motion of the magnets parallel or normal to the relative velocity. Even now, no computer codes that have these capabilities are commercially available.

The investigation reported here focuses on the characteristics of intrinsic damping forces associated with magnetic suspension systems and, in particular, on attempts to provide further insight into the nature of the intrinsic, negative magnetic damping phenomenon. The approach used in this investigation is simulation with a computer model, based on the combined mechanical and electromagnetic equations of motion for a magnet array interacting with a guideway loop-coil array. The approach is ideally suited to this investigation because the induced eddy currents that give rise to the principal levitation and guidance forces, as well as the intrinsic damping forces, are naturally constrained to the geometry of the guideway's conductor loops.

2 General Concept

2.1 Energy Conversion in a Maglev System

A maglev vehicle moving along a guideway (Figure 1) constitutes a typical electromechanical energy-conversion system, in which the propulsive motor converts electrical energy from an external power source into other forms of energy. These forms are expressed in terms of the vehicle's six degrees of motion through the electromagnetic coupling between the vehicle magnets and guideway conductors. During this energy-conversion process, it is also fundamental for the vehicle-borne superconducting magnets (SCMs) or conventional magnets to provide the magnetic field necessary to excite guideway conductors. From the vehicle's point of view, as a result of vehicle-guideway magnetic coupling, the mechanical energy from the propulsive motor is converted into the following energy forms: the dissipating energy in the guideway conductors, the magnetic energy stored in the vehicle magnets and the guideway conductors, the potential energy increase, and the mechanical energy stored in vehicle motions in six degrees of freedom. This energy-conversion process can be represented by a block diagram, as shown in Figure 2.

Assume that a maglev vehicle has a total mass of m and carries l superconducting magnets interacting with n guideway coils. Letting I_s be the initial SCM current, i_s be the sth SCM current at any time, i_g and R_g be the current and resistance of the gth guideway coil, respectively, and $L_{g,s}$ be the self or mutual inductance of the SCM or guideway coils, one can describe the energy conversion of a maglev system by the following equation:

$$\frac{1}{2}mv_x^2 + \frac{1}{2}\sum_{s=1}^{l} L_s I_s^2 = \int_0^t \sum_{g=1}^{n} R_g i_g^2 dt + \frac{1}{2}\sum_{g=1}^{n}\sum_{s=1}^{l} i_g i_s L_{g,s} + W_{mech,} \qquad (1)$$

where the first term on the left-hand side is the kinetic energy of the vehicle gained from the propulsive motor, the second term on the left-hand side is the initial magnetic energy stored in the SCMs aboard the vehicle, the first term on the right-hand side is the dissipated energy in the guideway coils, the second term on the right is the magnetic energy stored in the guideway coil-SCM-air gap system, and the last term on the right-hand side is the converted mechanical energy expressed in terms of the vehicle motions and the change in potential energy due to the change of air gap. The losses in the connecting cables and the aerodynamic drag forces are ignored for convenience.

Equation 1 indicates several important facts. First, the vehicle motion in any one direction is coupled with that in other directions through the magnetic energy stored in the air gap. Second, a maglev system, like any other conventional electrical machine, involves three forms of energy: electromagnetic, mechanical, and thermal energies. These energy forms must be balanced at any given time and can be transferred from one form to another. In particular, it should be noted that

the kinetic energy of the vehicle gained from the propulsive motor in the longitudinal direction can be transferred into the vertical, lateral, and other directions of the vehicle's motion.

2.2 Analogy between Mechanical and Electrical Systems and the Damping Concept

It is well known that a mechanical system can be analogous to an electrical system. For instance, a free-body motion system with a velocity v, having a mass of m, a damping constant of c, and a spring stiffness of k, can be analogous to an electrical circuit problem having an inductance L, a resistance R, and a capacitance C, as shown in Figure 3, because both systems have the same forms of differential equation—for the mechanical system

$$m\frac{dv}{dt} + \int kvdt + cv = f(t), \tag{2}$$

and for the electrical system

$$L\frac{di}{dt} + \frac{1}{C}\int idt + Ri = e(t), \tag{3}$$

where the mass m in the mechanical system is equivalent to the inductance L in the electrical system, the spring stiffness k is equivalent to the reciprocal of the capacitance C, the viscous damping constant c is equivalent to the resistance R, the applied force $f(t)$ is equivalent to the applied voltage source $e(t)$, and the velocity v is equivalent to the current i.

The power $p_e(t)$ delivered to the electrical system by the external voltage source $e(t)$ is obtained by multiplying Equation 3 by current i:

$$p_e(t) = e(t)i = \frac{d}{dt}\left(\frac{1}{2}Li^2\right) + \frac{i}{C}\int idt + Ri^2, \tag{4}$$

where the first and the second terms on the right-hand side are the rate changes of the energies stored in the inductance and capacitance, respectively; they are conservative terms. The last term represents the power dissipated in the resistance.

Similarly, in the mechanical system, the power $p_m(t)$ required to move a free body m at velocity v is given as

$$p_m(t) = f(t)v = \frac{d}{dt}\left(\frac{1}{2}mv^2\right) + v\int kvdt + cv^2, \tag{5}$$

where the first term on the right-hand side is the rate change of the kinetic energy of the system, the second term is the rate change of the energy stored in the spring, and the last term is the power dissipated due to damping constant c.

Note from Equations 4 and 5 that because the kinetic and potential energies in the mechanical system and the magnetic and electrical energies in the electrical system are conservative, the resistance R and the damping constant c are the only elements that absorb energy. A system is said to have positive damping if R, or c, is positive and to have negative damping if R, or c, is negative.

In general, there exists no negative resistance in a passive electrical network. However, an equivalent negative resistance can be defined for an active network if the network contains internal power sources and delivers power outside of the network, as shown in Figure 4. At this point, any external power source connected to the network may be considered to have negative damping because it absorbs energy from the network.

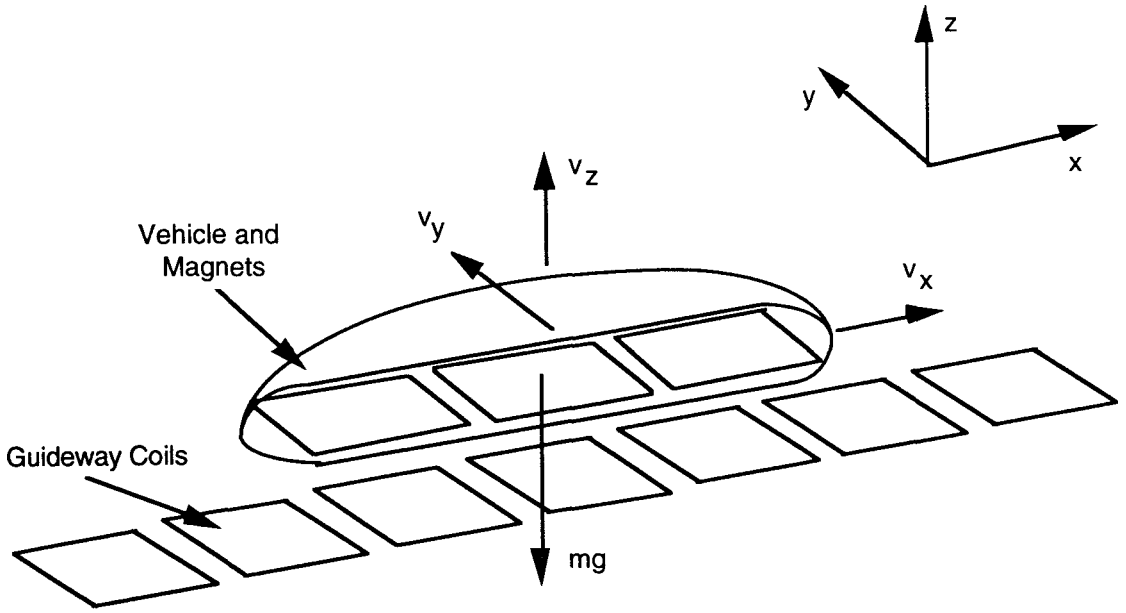

FIGURE 1 Sketch of a Maglev Vehicle Moving along a Loop-Coil Guideway

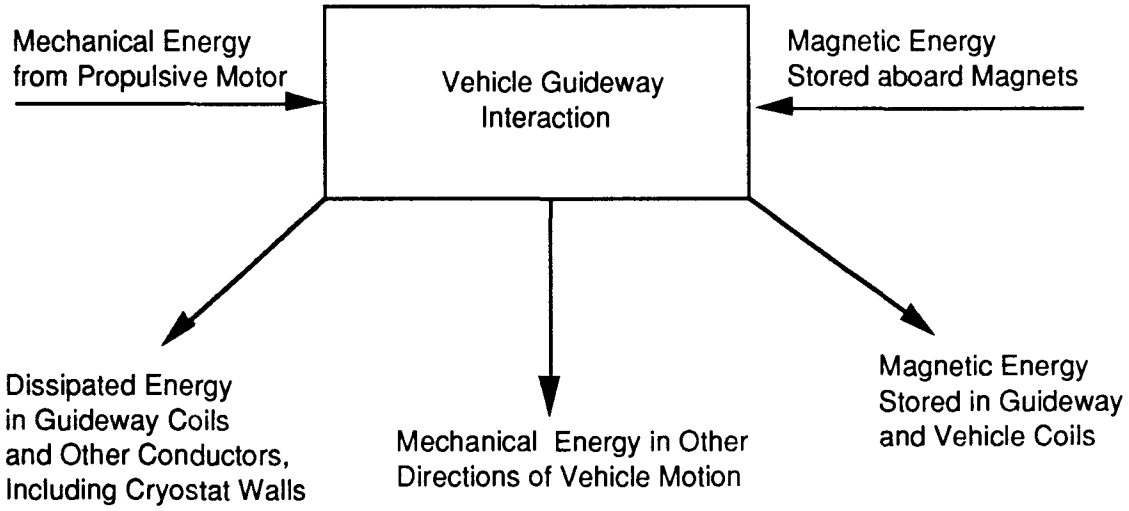

FIGURE 2 Energy Conversion in a Maglev System

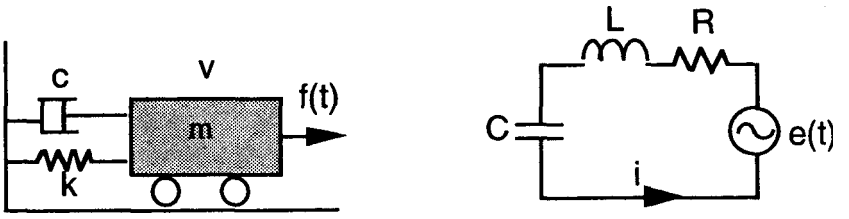

(a) Mechanical system (b) Electrical system

FIGURE 3 Analogy between Mechanical and Electrical Systems

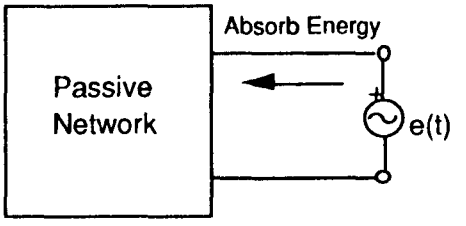

(a) A passive network absorbs energy from an external power source and shows no negative damping.

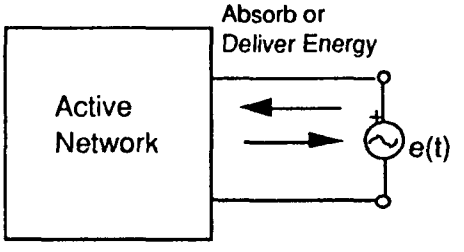

(b) An active network can deliver energy to an external power source, depending upon its internal configuration, and can show negative damping.

FIGURE 4 Network Presentation and Negative Damping Concept

3 Magnetic Damping in Maglev Systems

Magnetic damping, in contrast to most mechanical damping, results from the energy dissipation in an electrical circuit that is associated closely with the conversion of electromagnetic energy in the system. The nature of magnetic damping characteristics in a maglev system is of particular interest to many maglev designers. Negative damping characteristics will result in growing amplitude of the motion in one or more degrees of freedom of the vehicle, leading to instability of the maglev vehicle. It is essential to understand the mechanism of the magnetic damping force and to eliminate the instability caused by negative damping characteristics.

The simplest model for a maglev suspension system may be presented by a vehicle-borne, superconducting coil with a constant current I_s passing over a stationary guideway coil, as shown in Figure 5a, where the vehicle coil is assumed to move in three degrees of freedom, with x, y, and z being the displacements and v_x, v_y, and v_z, being the translation speeds, respectively. The system can be described by a dynamic circuit as shown in Figure 5b, where R and L are the resistance and inductance of the guideway coil and M is the mutual inductance between the vehicle coil and guideway coil. Note that M is a function of the displacements x, y, and z. A voltage equation can be written in terms of the current induced in the guideway as

$$L\frac{di}{dt} + iR + I_s v_x \frac{\partial M}{\partial x} + I_s v_y \frac{\partial M}{\partial y} + I_s v_z \frac{\partial M}{\partial z} = 0, \tag{6}$$

where the last three terms represent the voltages induced in the guideway coil due to vehicle motion in three directions. Let e_x, e_y, and e_z be the voltages induced in the guideway coil by the translation speeds v_x, v_y, and v_z, respectively:

$$e_x = - I_s v_x \frac{\partial M}{\partial x}, \tag{7}$$

$$e_y = - I_s v_y \frac{\partial M}{\partial y}, \tag{8}$$

and

$$e_z = - I_s v_z \frac{\partial M}{\partial z}. \tag{9}$$

Then Equation 6 can be rewritten as

$$L\frac{di}{dt} + iR = e_x + e_y + e_z. \tag{10}$$

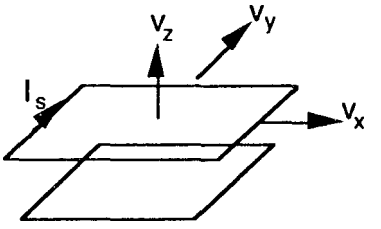

(a) A vehicle coil passing over a guideway coil

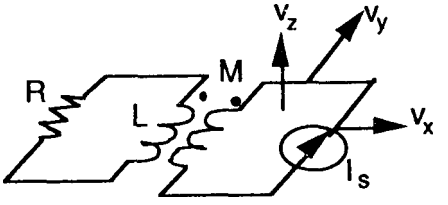

(b) Dynamic-circuit presentation

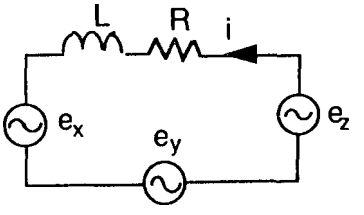

(c) Three voltage sources representing the vehicle motion in three directions

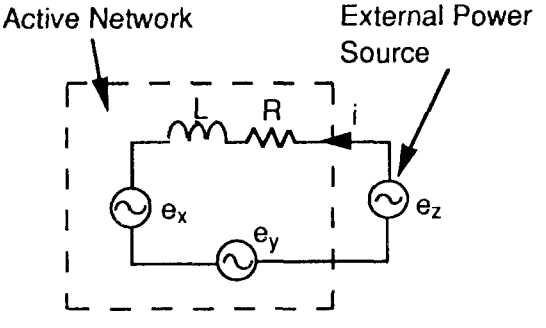

(d) The vertical motion is treated as an external power source; other motions are treated as part of the active network.

FIGURE 5 Dynamic-Circuit Presentation of a Vehicle Passing over a Guideway Coil

Equation 10 can be translated into an equivalent circuit as shown in Figure 5c, where the three voltage sources are connected in series with the other circuit elements. It is seen from Figure 5c that the power in one voltage source can be converted into other voltage sources through the current induced in the guideway coil (i.e., the current may have different phases relative to the voltage sources). Consequently, since each voltage source is related to a motion mode, the power associated with one motion mode can be converted into that of other motion modes through the energy stored in the air gap.

To understand the damping characteristics associated with the vertical motion, one can treat e_z as an external power source and e_x and e_y as the internal power sources of an active network, as shown in Figure 5d. Thus, the power p_z delivered to the network by the external voltage e_z is obtained as

$$p_z = f_z v_z = e_z i = \frac{d}{dt}\left(\frac{1}{2} L i^2\right) + i^2 R - e_x i - e_y i, \tag{11}$$

where the power associated with the vertical motion is expressed in terms of both mechanical and electromagnetic quantities. That is, this power can be expressed either by the product of the vertical magnetic force f_z and speed v_z, or by the product of the voltage e_z and current i. Equation 11 shows that the power converted to the vertical motion is balanced by several terms: the rate of change of the energy stored in the guideway coil, the power dissipated in the resistance, the power converted from the longitudinal motion, and the power converted from the lateral motion. Clearly, the power associated with the vertical motion may be positive or negative, depending upon the power relations given by Equation 11. The vertical power term becomes negative if the power inputs from the longitudinal and lateral motion modes are bigger than the power dissipated in the guideway coils. The negative value of p_z means that the force f_z and speed v_z are out of phase by 180°, which represents the negative damping force existing in the system.

The two-coil model developed here can also be applied to a real maglev system involving many vehicle and guideway coils. In this case, the inductance L in Figure 5 should be modified to take into account the coupling between the neighboring guideway coils. In addition, the mutual inductance M between one loop coil and one vehicle coil should also be modified to consider the coupling from all other vehicle coils. For instance, in a system having l alternating-pole SCMs interacting with a loop coil, the mutual inductance can be expressed as

$$M = \sum_{i=1}^{l} (-1)^i f[(x - i\tau), y, z)], \tag{12}$$

where f(x,y,z) stands for a general expression of the mutual inductance between one vehicle coil and one guideway coil and τ is the pole pitch of the vehicle magnet.

4 Computer Model Simulation of Nonsteady-State Response of Maglev Suspension System

4.1 The Model

The simple circuit model discussed in Section 3 is useful for determining some basic relationships, associated with the power and energy conversion of the system, that aid in understanding the mechanism of the magnetic damping phenomenon in a maglev system. However, to conduct real-time modeling of the magnetic damping force, a more complicated model becomes necessary. The new model developed in this section is able to describe a maglev system involving many vehicle-borne SCMs dynamically coupled with the guideway, in which the number of guideway coils is well-matched with the simulation distance and time. The model combines the electromagnetic system equations with the equations of motion and simulates the magnetic damping force and power in the time domain.

Consider a maglev vehicle that carries l vehicle-borne, superconducting coils with total mass of m and moments of inertia with respect to three axes J_x, J_y, and J_z, respectively, and that interacts with a loop-shaped, coil guideway in which n guideway coils are coupled with the vehicle coils. Let v_x, v_y, and v_z be the three translational speeds and ω_x, ω_y, and ω_z be the three rotational speeds of the vehicle. The system involves both electromagnetic and electromechanical quantities, interrelationships between which are governed by a complex set of coupled differential equations that, in general, cannot be solved analytically. Consequently, computer model simulation of nonsteady-state response is necessary to predict the vehicle's response to any perturbing forces. The system involves n equations for the current induced in the loop coils and 12 equations associated with vehicle motion in six degrees of freedom. The matrix equations for the currents induced in the guideway coils are obtained from Kirchhoff's voltage law:

$$[R][i] + [L]\frac{d}{dt}[i] + v_x I_s \frac{\partial}{\partial x}[M] + v_y I_s \frac{\partial}{\partial y}[M] + v_z I_s \frac{\partial}{\partial z}[M] +$$

$$\omega_x I_s \frac{\partial}{\partial \theta_x}[M] + \omega_y I_s \frac{\partial}{\partial \theta_y}[M] + \omega_z I_s \frac{\partial}{\partial \theta_x}[M] = 0, \qquad (13)$$

where [R] is a diagonal matrix containing n guideway coil resistances, [L] is a square (n by n) matrix containing self and mutual inductances of the guideway coils, [i] is a column matrix containing n unknown guideway coil currents, and [M] is a (l *by* n) matrix containing the mutual inductances between the superconducting coils and the guideway coils. The current I_s in the superconducting coils is assumed to be constant for all the coils. Note that the mechanical quantities associated with vehicle motions appear in Equation 13, which implies that the electrical system equations cannot be solved independently of the mechanical equations of motion.

The mechanical motion equations are also coupled with the electromagnetic quantities. For instance, the longitudinal acceleration is controlled by the applied propulsion force F_p (which in

turn depends on the current in the propulsion windings) minus the aerodynamic drag F_{ad} and the longitudinal magnetic force component (which depends on the current in the guideway conductors):

$$m\frac{dv_x}{dt} = F_p - \sum_{j=1}^{n}\sum_{s=1}^{l} I_s i_j \frac{\partial M_{s,j}}{\partial x} - F_{ad} \quad (14)$$

The vertical acceleration is determined by the vertical magnetic force component minus the gravitational force *mg*:

$$m\frac{dv_z}{dt} = \sum_{j=1}^{n}\sum_{s=1}^{l} I_s i_j \frac{\partial M_{s,j}}{\partial z} - mg \quad (15)$$

All other directions of motion are determined by the magnetic force components only:

$$m\frac{dv_y}{dt} = \sum_{j=1}^{n}\sum_{s=1}^{l} I_s i_j \frac{\partial M_{s,j}}{\partial y}, \quad (16)$$

$$J_x\frac{d\omega_x}{dt} = \sum_{j=1}^{n}\sum_{s=1}^{l} I_s i_j \frac{\partial M_{s,j}}{\partial \theta_x}, \quad (17)$$

$$J_y\frac{d\omega_y}{dt} = \sum_{j=1}^{n}\sum_{s=1}^{l} I_s i_j \frac{\partial M_{s,j}}{\partial \theta_y}, \quad (18)$$

and

$$J_z\frac{d\omega_z}{dt} = \sum_{j=1}^{n}\sum_{s=1}^{l} I_s i_j \frac{\partial M_{s,j}}{\partial \theta_z}. \quad (19)$$

Finally, the equations describing the relation between vehicle speeds and displacements are

$$v_x = \frac{dx}{dt}, \quad v_y = \frac{dy}{dt}, \quad v_z = \frac{dz}{dt},$$

$$\omega_x = \frac{d\theta_x}{dt}, \quad \omega_y = \frac{d\theta_y}{dt},$$

$$\text{and } \omega_z = \frac{d\theta_z}{dt}. \tag{20}$$

The system has n+12 unknowns and can be uniquely determined by the n+12 first-order differential equations described in Equations 13 through 20.

4.2 Numerical Results and Discussion

During the investigation into the characteristics of magnetic damping forces in the coil guideway, Equations 13 through 20 were solved numerically for various cases. Table 1 shows the dimensions and other parameters of a maglev system used in the simulations. In particular, the cases with one and two SCMs moving along a coil guideway were emphasized during the time-dependent modeling. For simplicity, rotational and lateral motions were neglected during the simulation. The investigation was focused on the coupling between longitudinal and vertical motions.

Initially, n guideway coil currents were assigned to be zero, and a levitation air gap was assumed. The vehicle was assumed to travel above the guideway at a given longitudinal speed v_x. Because the initial levitation gap was not equal to the value at equilibrium, the vehicle oscillated vertically, according to the nature of the magnetic force, while it traveled along the guideway. Time-dependent magnetic force components, power components associated with each motion mode, speeds, and displacements were obtained during the time-domain simulation.

In the selection of reasonable initial values for the simulation, the time-averaged lift and drag forces (as a function of longitudinal speed for the system given in Table 1) were calculated first (Figure 6). The lift force acting on the two magnets at an air gap of 20 cm was greater than 50 kN for longitudinal speeds higher than 20 m/s. The guideway coil had a time constant of 88 ms and a maximum lift-to-drag ratio of about 30. Thus, the system could generate a sufficient lift force to lift a six-metric-ton vehicle.

Figures 7 through 9 show a simulation case in which a six-metric-ton vehicle with two SCMs traveled a distance of 58 m along the guideway at a velocity of 10 m/s. The air gap was assumed to be 16 cm initially and approached 15 cm at the end of the simulation, as shown in

TABLE 1 Data Used for Numerical Example

Parameter	Value
Loop Coil	
Length (m)	0.5
Width (m)	0.5
Conductor cross section (cm^2)	80
Conductivity ($m^{-1}\ \Omega^{-1}$)	3×10^7
Space between two coils (m)	0.1
Superconducting Coil	
Length (m)	1.5
Width (m)	0.5
Magnetomotive force (kA·T)	200
Vehicle Mass (kg)	6,000

Figure 7. This initial vertical perturbation produced a vertical oscillation with a maximum vertical speed smaller than 0.1 m/s. The vehicle oscillated vertically for about 10 periods within about 5.8 seconds, corresponding to a 58-m distance of travel. This gave a vertical oscillation frequency of 1.72 Hz.

Figure 8 shows the lift and longitudinal force components as a function of time, where both force components involve high-order harmonics associated with the discrete coil guideway. It will be shown later that these high-order harmonics can be reduced by changing the ratio of the pole pitch of the vehicle magnets to the coil pitch of the guideway. The time-averaged value of the longitudinal force component in Figure 8 is the magnetic drag in the system. Note from Figures 7 and 8 that the force components, levitation air gap, and vertical speed all oscillated at the same frequency and decayed at the same time constant. From these waveform profiles, the damping factor of the system at 10 m/s was calculated to be 0.043.

Figure 9 shows the time-dependent power terms related to the longitudinal and vertical motions and the power dissipated in the resistance. The negative value of the power waveform, corresponding to the longitudinal motion, represents the power obtained from the propulsion motor. The longitudinal power waveform consists of two parts: the dissipative part, corresponding to the resistance, and the conservative part, associated with the rate change of the stored magnetic energy. The time-averaged value of the longitudinal power term is equal to the power dissipated in the electromagnetic force or resistance, because the conservative part vanishes after time-averaging. It is important to note from Figure 9 that the vertical power term is very small, only a small percent of the resistive power. The vertical power term vanishes after several oscillation periods because, in this case, the system absorbs energy and displays positive damping characteristics.

The simulations were conducted for various longitudinal speeds. The results show that the damping factor decreases as the longitudinal speed increases, becoming negative for longitudinal speeds higher than 18 m/s.

Figure 10 shows a simulation case in which the vehicle traveled a distance of 120 m at a longitudinal speed of 25 m/s. The initial levitation gap was selected to be 0.2 m, because the time-averaged lift force increased at the speed of 25 m/s. In this case, the amplitude of the lift force, vertical speed, and levitation air-gap waveforms grew slowly as the vehicle traveled along the guideway. The damping factor corresponding to the longitudinal speed of 25 m/s was calculated from Figure 10 to be -0.0015. This implies that a very small amount of power was transferred from the longitudinal motion mode to the vertical mode. In other words, the vertical motion mode absorbed energy from the system, which is equivalent to saying that the system had negative damping characteristics. With respect to the system depicted in Figure 5d, the network would be feeding energy into the external power source, represented by the voltage term e_z.

Figure 11 shows the damping factor as a function of longitudinal speed, with the number of magnets as a parameter. For the two-magnet case, the damping factor decreased rapidly for longitudinal speeds lower than 10 m/s and changed slowly to the negative for speeds higher than 18 m/s. This factor reached a maximum negative value at about 25 m/s and finally approached zero at higher speeds. This is consistent with the results discussed in Reference 3, where the fundamental wave was assumed. Note that the case of a single magnet moving along the guideway showed no negative damping phenomenon. Figure 12 shows a case where a single SCM, weighing three metric tons, moved along a guideway at a longitudinal speed of 25 m/s. The lift force, vertical speed, and air gap decayed slowly as the vehicle moved forward, and the magnet did not show any negative damping characteristics. This implies that the negative damping characteristic depends upon the space harmonics. The single-magnet system has stronger end effects compared with those of a double-magnet system, and this changes the coupling between the motion modes. At this point, it is clear that the model developed in Reference 3, on the basis of the fundamental wave alone, is not suitable for the single-magnet problem.

To demonstrate the sensitivity of the harmonics resulting from the discrete coil guideway, additional simulations were conducted that varied the coil pitch of the guideway. The simulation results for a typical case, with a coil length of 0.4 m at a longitudinal speed of 10 m/s, are shown in Figures 13 through 15, where the harmonics associated with the discrete coil guideway are reduced substantially. In this case, the time constant of the guideway coil was reduced to 82 ms and the damping factor was 0.036, because both the resistance and inductance of the guideway coil were reduced. The curves describing the damping factor as a function of vehicle speed in Figure 11 are expected to shift slightly to the left.

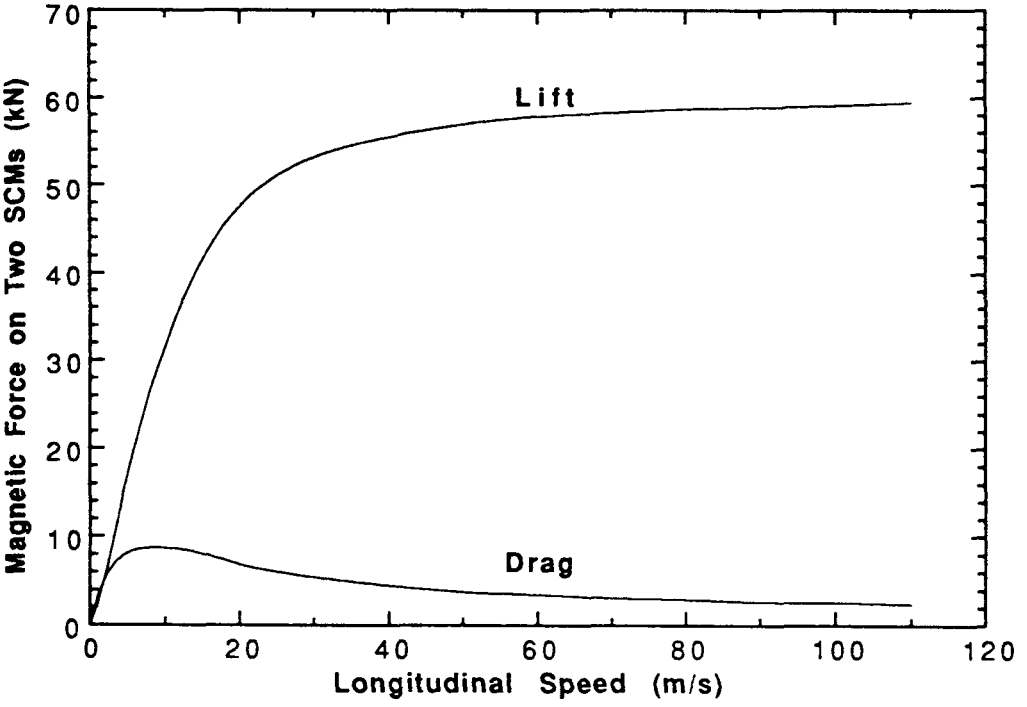

FIGURE 6 Time-Averaged Magnetic Force as a Function of Speed (air gap: 20 cm; see Table 1 for other parameters)

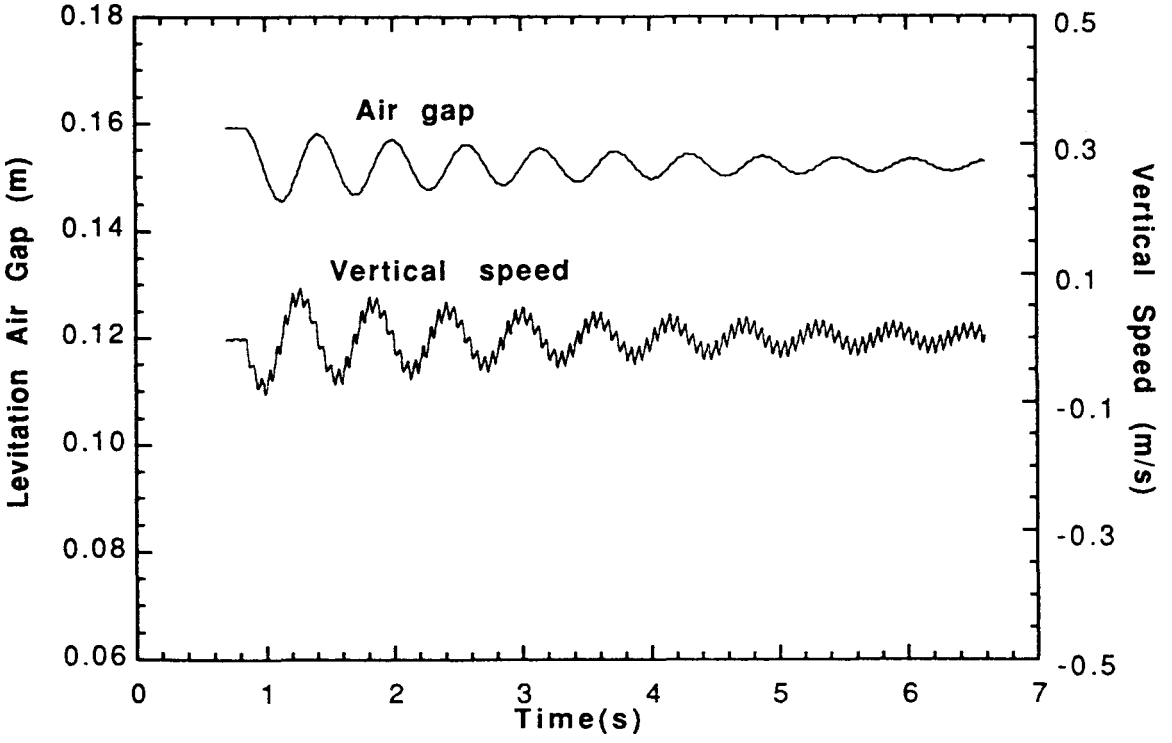

FIGURE 7 Vertical Speed and Air Gap as Functions of Time (loop coil: 0.5 m by 0.5 m; vehicle speed: 10 m/s)

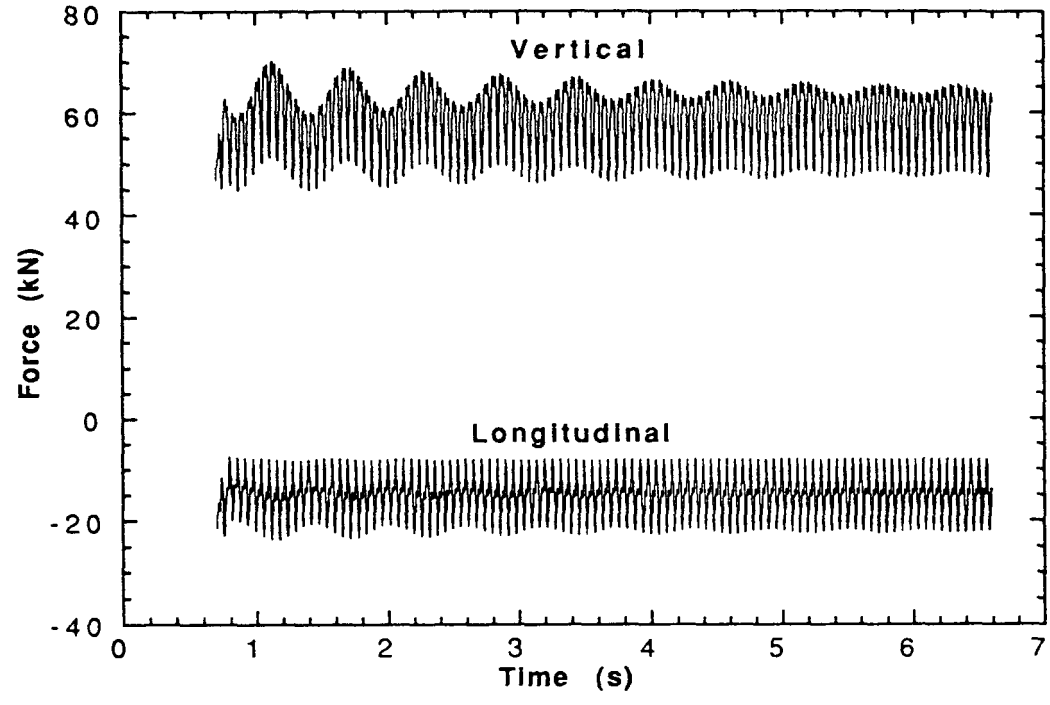

FIGURE 8 Vertical and Longitudinal Forces as Functions of Time (coil length: 0.5 m by 0.5 m; vehicle speed: 10 m/s)

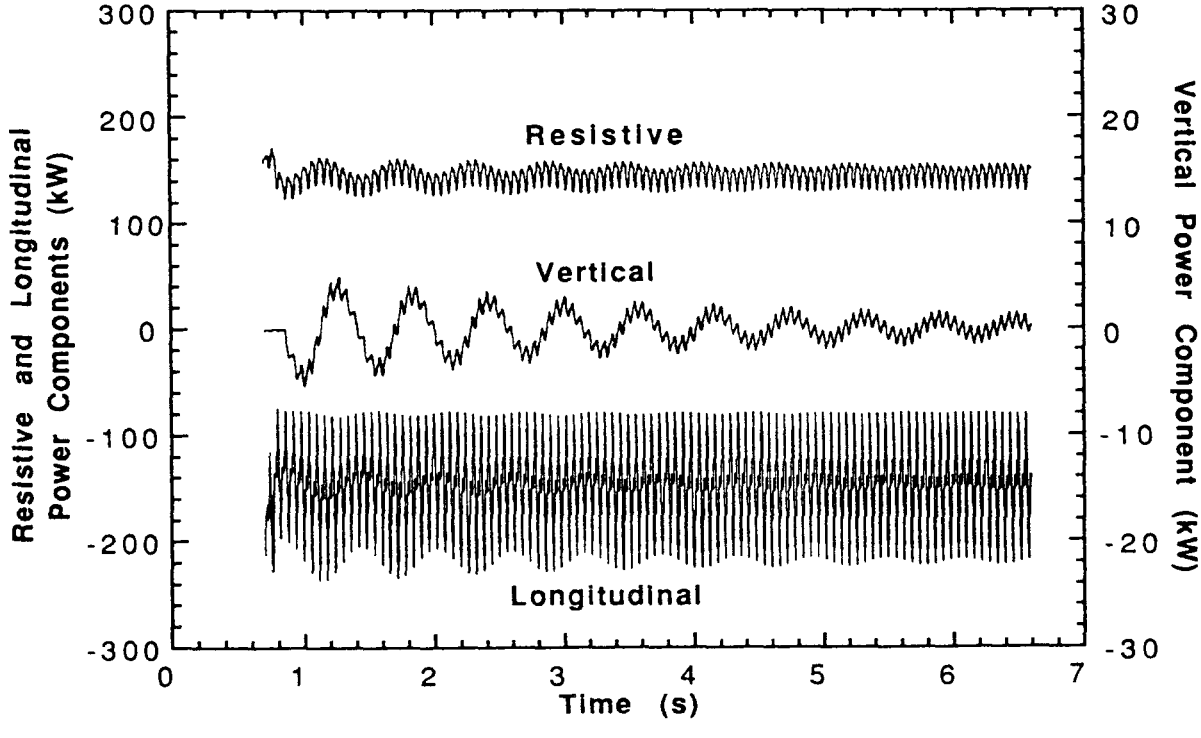

FIGURE 9 Power Waveforms (loop coil: 0.5 by 0.5 m; vehicle speed: 10 m/s)

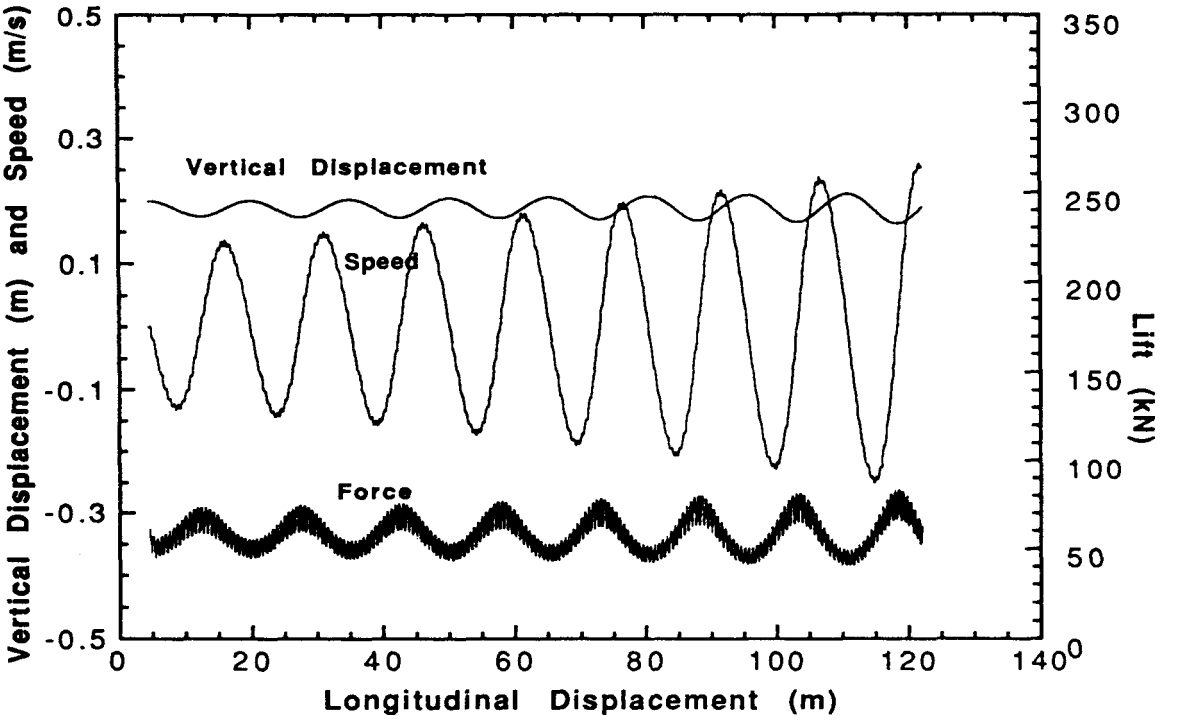

FIGURE 10 Lift-Force, Air-Gap, and Vertical-Speed Waveforms (loop coil: 0.5 m by 0.5 m; vehicle speed: 25 m/s)

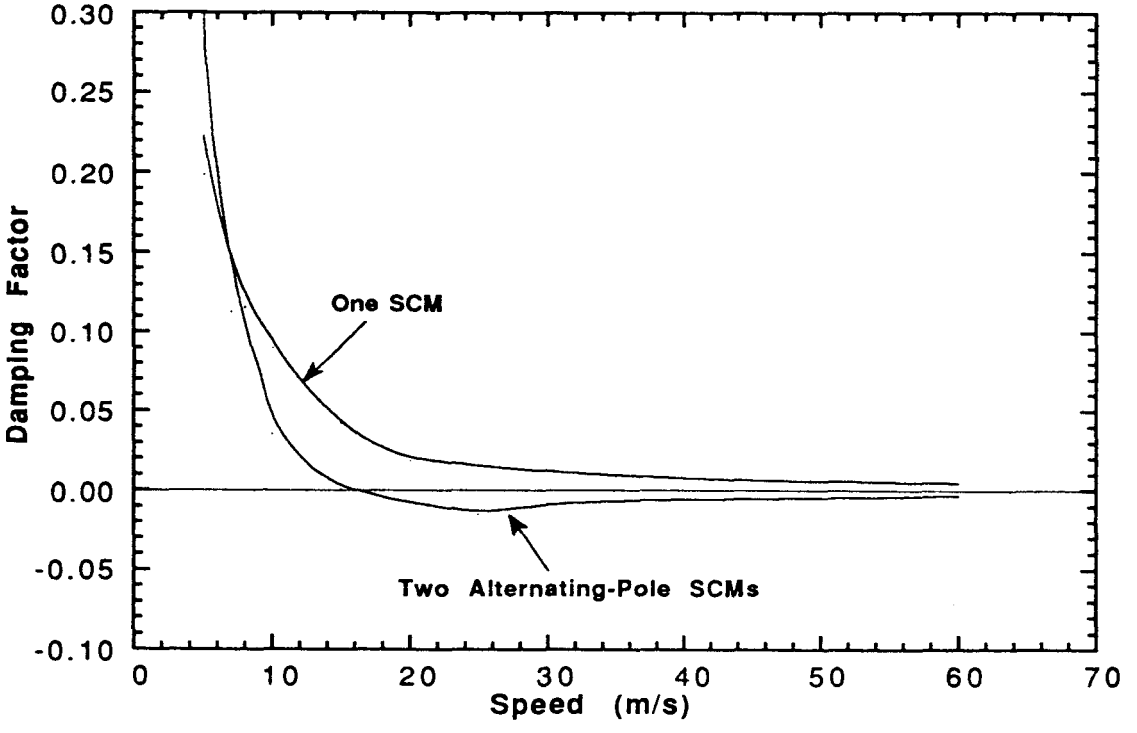

FIGURE 11 Magnetic Damping Factor as a Function of Vehicle Speed (SCM: 1.5 m by 0.5 m; loop coil: 0.5 m by 0.5 m, with a gap of 0.1 and a time constant of 0.0877 s)

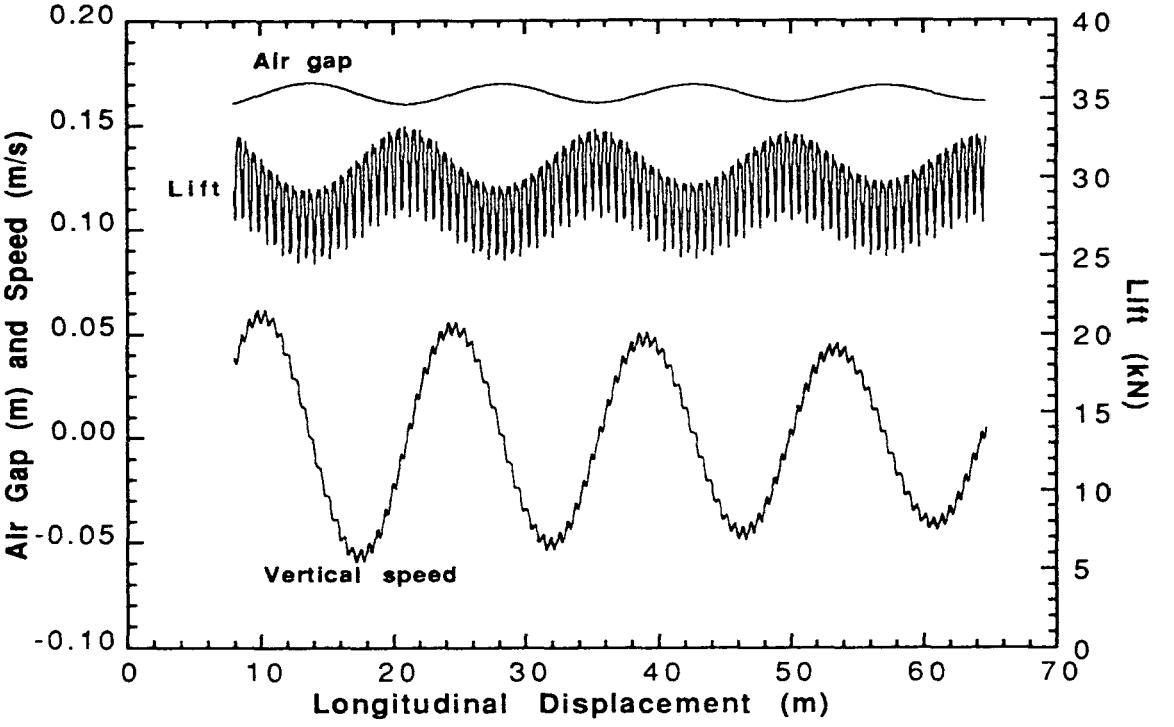

FIGURE 12 Single Superconducting Magnet Moving above Loop-Coil Guideway (vehicle speed: 25 m/s; loop coil: 0.5 m by 0.5 m)

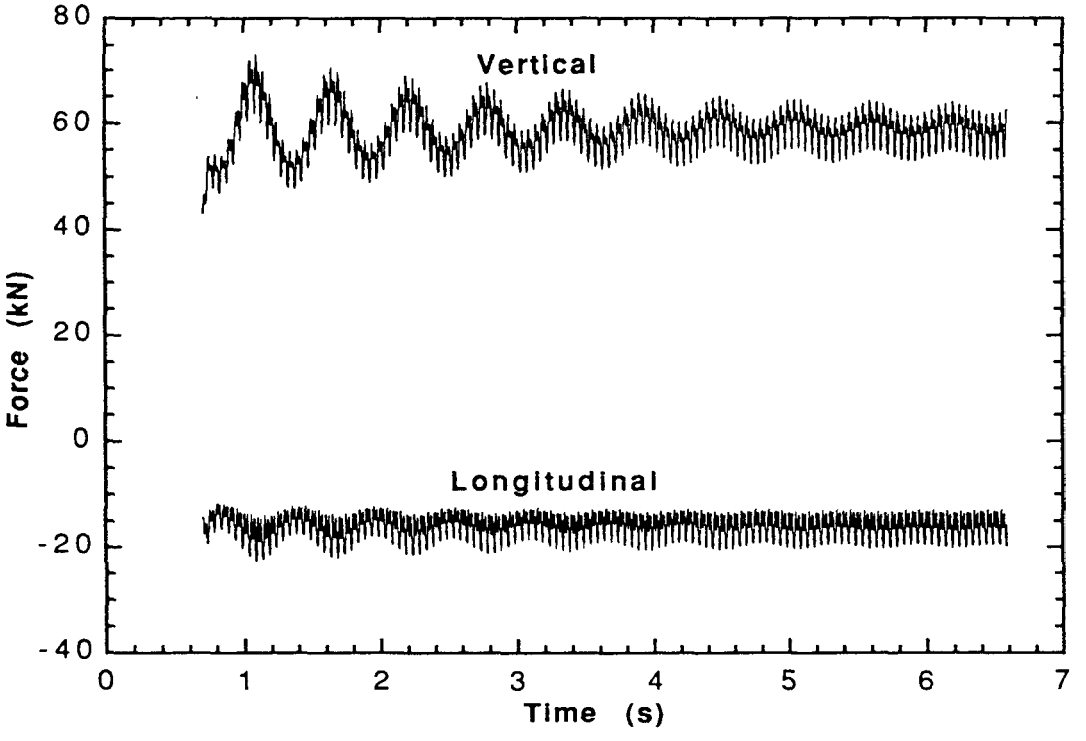

FIGURE 13 Force-Component Waveforms (loop coil: 0.4 by 0.5 m; vehicle speed: 10 m/s)

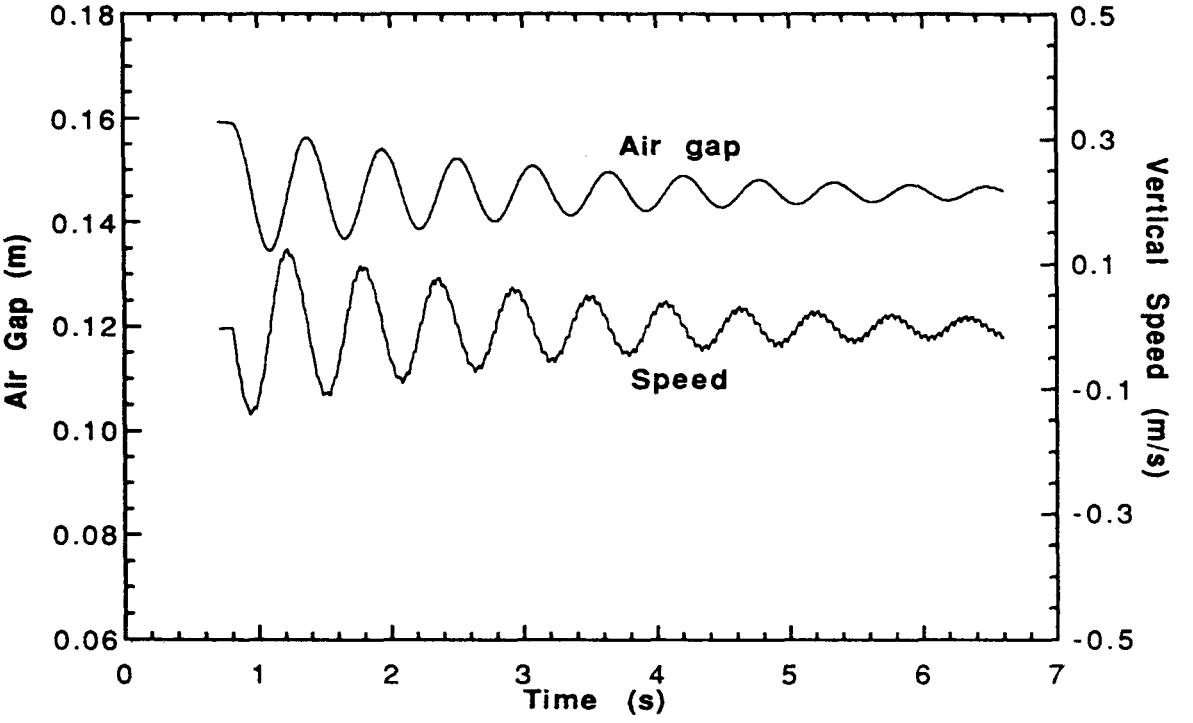

FIGURE 14 Air Gap and Vertical Speed as Functions of Time (vehicle speed: 10 m/s; loop coil: 0.4 by 0.5 m)

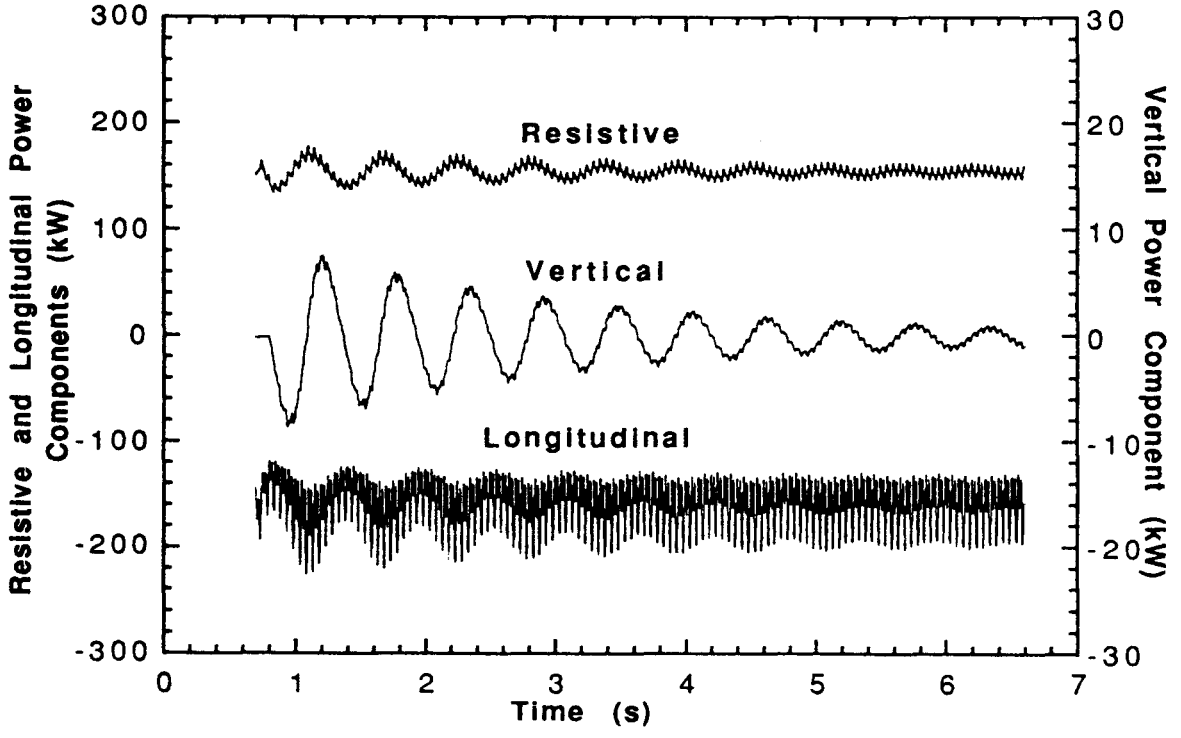

FIGURE 15 Power-Component Waveforms (vehicle speed: 10 m/s; loop coil: 0.4 by 0.5 m)

5 Conclusions

A simple circuit model was developed for the understanding of magnetic-damping-force characteristics in the maglev system. The model treats each motion mode as a voltage source connected in series with other modes. Thus, a maglev system, in which the energy in one motion mode is transferred to other motion modes through the magnetic energy stored in the air gap, is described by a circuit, in which the power in one source is transferred to other sources through the current induced in the guideway coils. The negative damping force associated with the vertical motion arises simply because the power in the propulsion model is converted to the vertical mode.

A computer simulation model that combined both electromagnetic- and mechanical-system equations was developed for the investigation of the magnetic damping characteristics. Time-dependent magnetic forces, powers, and other electromechanical quantities were simulated for various cases, typically focusing on the coil guideway. Results confirmed the existence of the negative damping phenomenon in the coil guideway. However, the negative damping factor is relatively small. In a real maglev system, such a small, negative magnetic damping force can be overcome, most likely, by the eddy current losses in many mechanical components and the aerodynamic drag, which were not considered in the computation. The simulations also show that a single magnet moving above a coil guideway does not display any negative damping force. It seems that the space harmonics associated with end effects play an important role in the negative damping phenomenon: the more important the end effects are, the less important the negative damping effect would appear to be; further investigation of this phenomenon is needed. Finally, it was found that a proper selection of the ratio of pole pitch to coil pitch seems to be very important in reducing force oscillations that result from the discrete-coil nature of the guideway.

Further investigation on this subject should focus on the dimensional dependence of the negative damping characteristics, such as the effects of pole pitch, coil pitch, number of SCMs, and space between the coils, on the damping forces.

6 References

1. Moon, F.C., 1977, "Vibration Problems in Magnetic Levitation and Propulsion," chap. 6 in *Transportation without Wheel,* E.R. Laithwaite, Paul Elek Scientific Books, Ltd., pp. 123-161, London.

2. Davis, L.C., and D.F. Wilkie, 1971, "Analysis of Motion of Magnetic Levitation Systems: Implications for High-Speed Vehicles," *Journal of Applied Physics* 42(12):4779-4793, Nov.

3. Yamada, T., M. Iwamoto, and T. Ito, 1974, "Magnetic Damping Force in Inductive Magnetic Levitation System for High-Speed Trains," *Electrical Engineering in Japan* 94(1):49-54.

4. Fujiwara, S., and T. Hariyama, 1983, "Damping Characteristics and AC Magnetic Field of Repulsive Magnetic Levitation," *Japanese Railway Technical Research Institute, Quarterly Reports* 24(2):93.

5. Fujiwara, S., 1980, "Damping Characteristics of the Repulsive Magnetic Levitation Vehicle," *Japanese Railway Technical Research Institute, Quarterly Reports* 21(1):49-52.

6. Yamaguchi, H., and S. Fujiwara, 1993, "Influence of Current Model of SCM on Electromagnetic Damping of EDS Type Maglev," Proceedings of International Conference on Speedup Technology for Railway and Maglev Vehicles, Nov. 22-26, 1993, Yokohama, Japan, pp. 192-195.

7. Chen, S.S., S. Zhu, and Y. Cai, 1993, *On the Unsteady-Motion Theory of Magnetic Forces for Maglev,* Argonne National Laboratory Report ANL-93/39.

8. Ohsaki, H., et al., 1993, "Damping Characteristics of the Superconductive Maglev Vehicle," 6th International Symposium on Superconductivity, Hiroshima, Japan, Oct. 26-29.

9. Coffey, H.T., 1974, "SRI Magnetic Suspension Studies for High-Speed Vehicles," *Advances in Cryogenic Engineering, Vol. 19,* Plenum Press, New York and London, pp. 137-152.